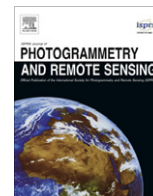


Contents lists available at [SciVerse ScienceDirect](http://www.sciencedirect.com)

ISPRS Journal of Photogrammetry and Remote Sensing

journal homepage: www.elsevier.com/locate/isprsjprs

Shanghai subway tunnels and highways monitoring through Cosmo-SkyMed Persistent Scatterers

Daniele Perissin^{a,1}, Zhiying Wang^{b,*,2}, Hui Lin^a

^a Chinese University of Hong Kong, Shatin, Hong Kong

^b Politecnico di Milano, Milan, Italy

ARTICLE INFO

Article history:

Available online 6 September 2012

Keywords:

Persistent Scatterers
Urban subsidence monitoring
Subways
Highways
Shanghai

ABSTRACT

Synthetic Aperture Radar Interferometry (InSAR) is an alternative technique to obtain measurements of surface displacement providing better spatial resolution and comparable accuracy at an extremely lower cost per area than conventional surveying methods. InSAR is becoming more and more popular in monitoring urban deformations, however, the technique requires advanced tools and high level competence to be successfully applied. In this paper we report important results obtained by analyzing new high resolution SAR data in the Shanghai urban area. The data used in this work have been acquired by the Italian X-band sensor Cosmo-SkyMed. About 1.2 million of individual and independent targets have been detected in 600 sq km, revealing impressive details of the ground surface deformation. Using the SAR-PROZ InSAR tool and integrating the results with Google Earth, we were able to track subway tunnels recently excavated and several highways. Tunnels are visible due to very localized subsidence of the above surface along their path. On the other hand, highways, standing over the ground, in most cases show higher stability than the surrounding areas. The density of targets is so high to allow studying the profile of the tunnel subsidence, which is very useful to predict building damage. Finally, the identification of targets on high buildings helps checking the stability of high constructions along the subway lines, highlighting possible risky situations.

© 2012 International Society for Photogrammetry and Remote Sensing, Inc. (ISPRS) Published by Elsevier B.V. All rights reserved.

1. Introduction

1.1. Shanghai subway development

Shanghai, as one of the most populated cities in the world, made an enormous effort in expanding its underground railway network. In particular, in the six months leading up to the opening of the Expo on May 1, 2010, the Shanghai Metro has undergone major expansions (Miller et al., 2010). Three new lines, one temporary new line and two extensions became functional before the Expo event. The incredibly rapid development generated also crit-

ics concerning safety, strengthened by the accident happened on September 27, 2011 along line 10 (Mu, 2011).

From 1995 to April 2010, Shanghai has increased the subway network from one single line to 12, 268 stations in total and 420 km in length. Moreover, the system is still under development. According to the last reports, by the end of 2020 Shanghai plans to extend the subway network to a total number of 22 lines, spanning almost 900 km. The ambitious project awakens big expectations for the population, but at the same time it rises concerns about safety and possible subsidence risks.

1.2. Subsidence monitoring in Shanghai

Shanghai is located on the deltaic deposit of the Yangtze River. Compaction of the 40-m-thick, upper Shanghai soft clay contributes to land subsidence in the Shanghai region (Gong et al., 2009). A lot of attention has been paid to the subsidence caused by the groundwater pumping since 1921 (Damoah-Afari et al., 2007, 2008; Hu et al., 2004; Monjoie et al., 1992; Shi and Bao, 1984). However, the subsidence in urban area could also be caused by many other anthropogenic factors, such as construction

* Corresponding author.

E-mail addresses: daniele.perissin@cuhk.edu.hk (D. Perissin), zhiying.wang@mail.polimi.it, wzy_sc@sina.com (Z. Wang).

¹ Institute of Space and Earth Information Science – ISEIS, Chinese University of Hong Kong – CUHK, Fok Ying Tung Remote Sensing Science Building, CUHK, Shatin, New Territories, Hong Kong.

² Received her Ph.D degree in mechanical engineering system from Politecnico di Milano in February 2010 and mechatronics from Beijing University of Astronautics and Aeronautics in July 2010. She is now working on InSAR and Robotics.

of high rise buildings, subways excavation and so forth. A large amount of people (Shanghai population is more than 18 million) travels by metro and moves via subways everyday. The terrain surface is disseminated of high-rise sky scrapers, that pierce a network of highways and bridges. Subsidence caused by excavation could thus cause disasters endangering the life of many people.

The bury-depth of most metro tunnels in Shanghai is limited because of the special soil condition. Most tunnels pass through very soft clay and very soft silty clay levels. Such kinds of clay have properties as large void ratio, high water content, high plasticity, poor permeability, high compressibility, low shearing strength and low modulus of deformation (Hu et al., 2003), which lead to high probability of subsidence (Tang et al., 2008; Wei et al., 2011; Yang et al., 2010). Shanghai's responsible offices spent a considerable amount of money for installing different kind of instruments to monitor the stability of the terrain in construction areas (Shanghai.gov.cn, 2007; Water news Online, 2007). Even though, it is impractical to install sensors along all tunnels, and thus it is impossible to have a detailed and global vision at the same time with common surveying methods.

Synthetic Aperture Radar Interferometry (InSAR) can provide alternative measurements of the surface displacement with better spatial resolution and comparable accuracy than conventional surveying methods, allowing to study vast areas at once (Osmanoğlu et al., 2010). In particular, the Permanent Scatterers InSAR technique (PSInSAR) (Ferretti et al., 2000), which was introduced and developed at Politecnico di Milano (POLIMI) in the late 1990s, is a highly efficient tool for investigating the subsidence pattern of stable radar targets. The aim is achieved by processing series of images and reducing, in this way, the effect of decorrelation (which makes the interferometric phase random) and atmosphere (which biases the movement estimated from the interferometric phase). InSAR has already been applied in different sites in China, as Tianjing, Shanghai, Suzhou, Wuhan (Damoah-Afari et al., 2008; Li et al., 2009; Liu et al., 2009; Perissin and Wang, 2010). As an example, in (Perissin and Wang, 2010) we published a PSInSAR analysis in Shanghai carried out with 40 ESA-ERS images acquired between 1993 and 2000. The results were compared with optical leveling measurements collected from 1990 to 1998, showing a good agreement.

Meanwhile, new high resolution satellites (like the German TerraSAR-X and the Italian Cosmo-SkyMed) have been launched in orbit, opening to new horizons in monitoring urban areas with InSAR techniques. The availability of archives of X-band data makes it now possible to apply successfully multi-image processing analysis for high resolution land subsidence monitoring. In particular, in this work Cosmo-SkyMed data acquired over Shanghai and provided by Eastdawn, Beijing were processed with the PSInSAR technique.

1.3. The SARPROZ InSAR tool for urban subsidence

Different software tools are nowadays available for applying multi-image InSAR techniques. In this work we make use of SARPROZ, a program developed by Perissin. SARPROZ (Perissin et al., 2011; Perissin, 2011) is a versatile software for processing SAR and InSAR Data. Programmed in Matlab, it offers easy ways to extend the existing library of functions. At the same time, it is based on graphical interfaces and it can be used without coding knowledge (examples in Fig. 1). Moreover, it is completely parallelized and, thanks to the powerful Matlab libraries, it can run automatically on multiple processors or computer clusters. The tool implements various kinds of multi-temporal techniques, as PS and Quasi-PS (Ferretti et al., 2001; Perissin and Wang, 2012), and any

kind of multi-master interferometric combination and stacking. The software provides modules for coherent–incoherent processing, including multi-platform data combination, time series analysis (both of phase and amplitude data), DEM–DSM analysis, target characterization and classification, change detection. The software offers also several tools for data analysis, data plotting and data exporting in different formats including Google Earth (GE) (Perissin et al., 2011).

The advantages of using GE are its being free, its high browsing speed and its big images archive, with even historic information. However, when dealing with huge numbers of points (as in a PSInSAR analysis), some smart solutions have to be adopted in order not to overload the GE memory. SARPROZ implements two ways of results exportation to GE. In the first one, PS results are re-sampled on a uniform geographic grid, to give an overview of the estimated parameter without overloading the GE memory. At a second time, results can be displayed on a point-by-point basis, to make it possible browsing into all estimated details. Examples are reported in Section 3.

SARPROZ is not a commercial software and the source code is not public. The interested reader may contact the author (Perissin, 2011) on how to get the code for research purposes.

2. Data set and methodology

Thirty-three scenes acquired by Cosmo-SkyMed between December 2008 and June 2010 along an ascending orbit were used to carry out a PSInSAR analysis with SARPROZ. The processed area covers around 600 sq km, acquisitions are in Stripmap imaging mode (3 m resolution). The scene on 10th, October 2009 is chosen as reference (Master image) to minimize the effects of normal and temporal baselines (the higher the baseline, the higher is the impact of de-correlation (Zebker and Villasenor, 1992)). The interferometric configuration is shown in Fig. 2, where each point represents an image in the normal baseline/temporal baseline space and each link an interferogram. All interferograms are generated with respect to the Master image.

The technique used in this analysis is a classical InSAR multi-temporal processing, in which the adopted model of the deformation is linear in time. The only advanced options we selected are relative to the urban character of the analysis with high resolution SAR data:

1. Identification of independent targets (discarding dependent pixels) (Perissin and Rocca, 2006). This option is particularly useful to avoid ghost mislocated targets.
2. Estimation of double scatterers in a single resolution cell (Ferretti et al., 2005). The skyline of Shanghai often causes the mixing of reflections from building facades and ground targets. Without considering double scatterers, several buildings would not match the classic model for PSs and would be interpreted as noisy reflections.
3. Estimation of a seasonal trend for targets lying on high buildings (Perissin and Rocca, 2006). Long vertical structures are affected by thermal dilation. Without estimating and removing seasonal signals from phase series, the classic model for PSs would fail and high buildings would appear as noisy targets.
4. Estimation of target life time to detect also temporary targets (Colesanti et al., 2003). Though the time span of the analyzed data is short, Shanghai is developing at a very fast rate and new constructions would not be accounted as Permanent Scatterers without estimating their actual life time.

Beside the common results of the processing (average ground deformation trend and terrain height) it is worth to mention the

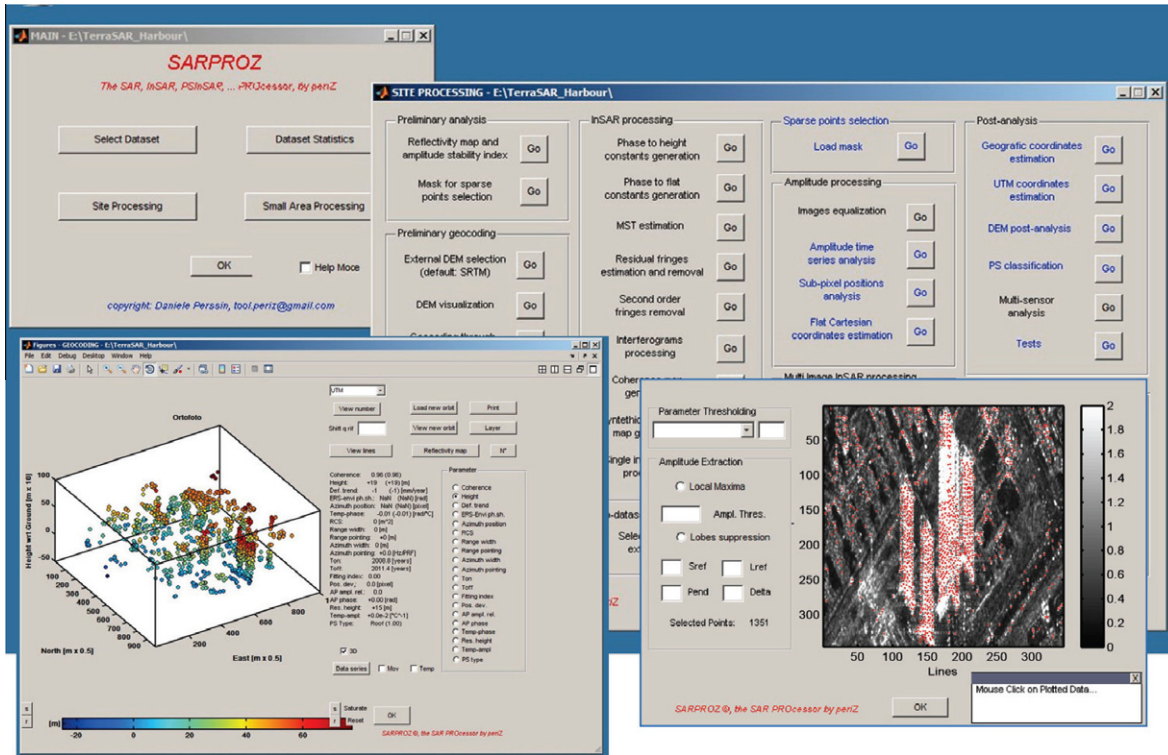


Fig. 1. Examples of the interface of the SAR processing tool SARPROZ.

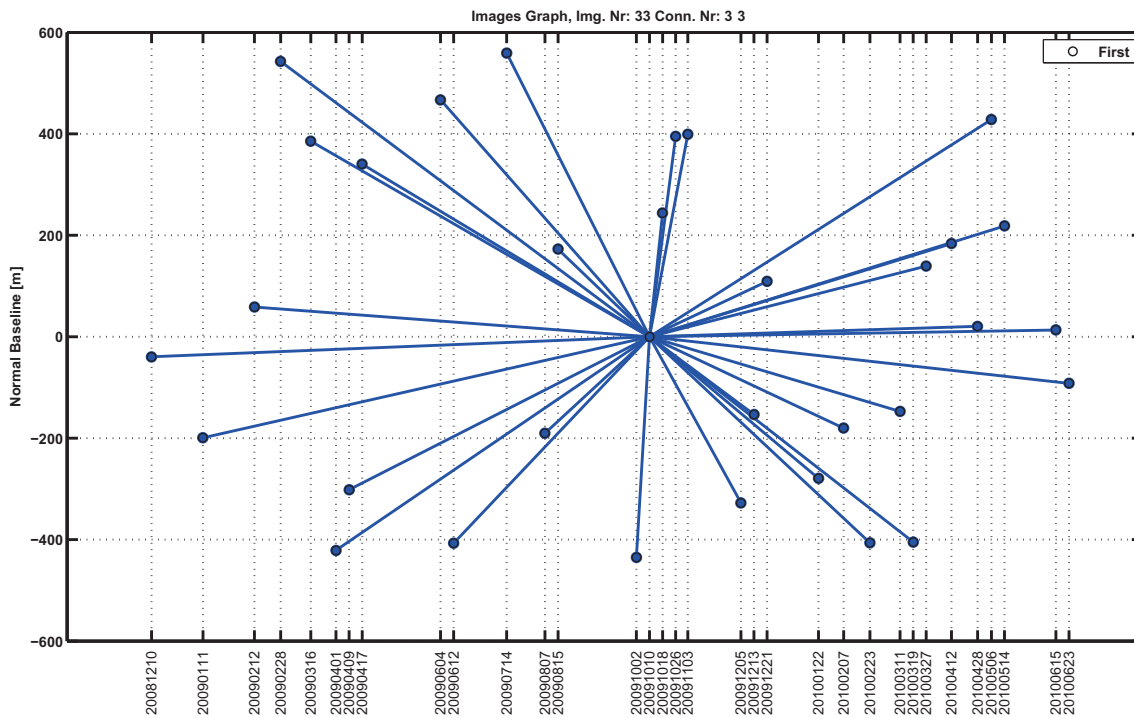


Fig. 2. Cosmo-SkyMed dataset analyzed in this work. Each point represents a image in the normal-temporal baseline space; each line represents an interferogram. The configuration corresponds to the single master PS analysis.

Atmospheric Phase Screen (APS) that we estimated in the area. It is known that Shanghai is characterized by strong humidity and X band is particularly sensitive to atmospheric delay due to

the short wavelength. Strong turbulence has been detected and removed by the multi-temporal processing, providing very interesting details of the concentration of water vapor in Shanghai.

The topic deserves further studies that we will report in future works. The estimated APS has been removed from data for obtaining time series of the displacement of targets.

3. Results and discussion

3.1. Overview

About 1.2 million independent targets have been detected in the studied area processing the Cosmo data-set with the technique mentioned in the previous section. Fig. 3 reports the main result of the work. In Fig. 3 two subsidence maps are presented: the first one, on the top, was estimated with ERS data acquired between 1993 and 2000; the second one, at the bottom, has been retrieved from the Cosmo data described in this work. In the first plot, the color scale is $[-40\ 40]$ mm/year, while the second one movements are displayed in a scale $[-25\ 5]$ mm/year. The two maps, reporting the average linear deformation trend, cannot be directly compared for several reasons: time span and time spacing between subsequent image are quite different, the displacement is measured along two different looking directions (ERS data are ascending, while Cosmo data are descending), reference points are different.

However, the comparison gives an idea of the evolution of the major subsidence centers passing from year 2000 to year 2010.

From Fig. 3 we can firstly notice that the two main macro-areas of subsidence are north of Hongqiao airport (on the left) and west of Huangpu river (Zhabei district, in the middle). The subsiding areas appear in red in the ERS map and in yellow/red in the Cosmo one. The subsidence is affecting the same macro-areas in the two maps, however, its magnitude and extension consistently reduced from year 2000 to year 2010. The Shanghai government is in fact spending great efforts in controlling ground movements, and it is known that the overall sinking is decreasing progressively (Gov.cn, 2011).

At the same time, Fig. 3 highlights a big difference between ERS and Cosmo data. While the ERS result is based on a quite sparse set of points, the Cosmo subsidence map is an almost continuous distribution of PSs. The increase of resolution of X band is generating a density of targets about 20 times the one of C band. It is nice to appreciate the precise alignment of PSs around features like water bodies, vegetated areas or airports.

The high density of detected PSs can be better observed from Fig. 4, where targets are displayed on a point-by-point basis. In Fig. 4 PSs are displayed in 3D and the color is proportional to the

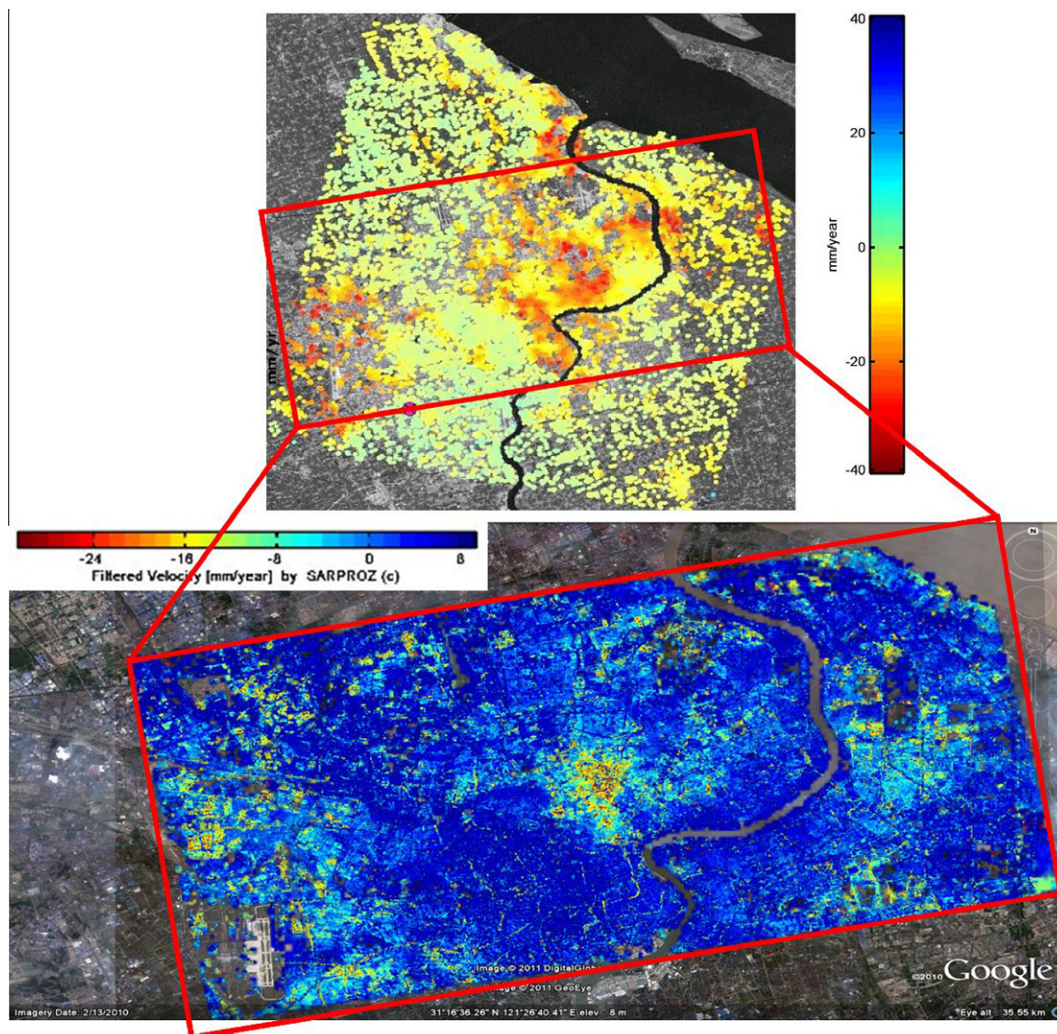


Fig. 3. Average deformation trend estimated by processing ERS data (upper image) and Cosmo-SkyMed data (lower image) over Shanghai with the PS technique. The color scales are $[-40\ 40]$ and $[-25\ 5]$ mm/year respectively. (For interpretation of the references to color in this figure legend, the reader is referred to the web version of this article.)

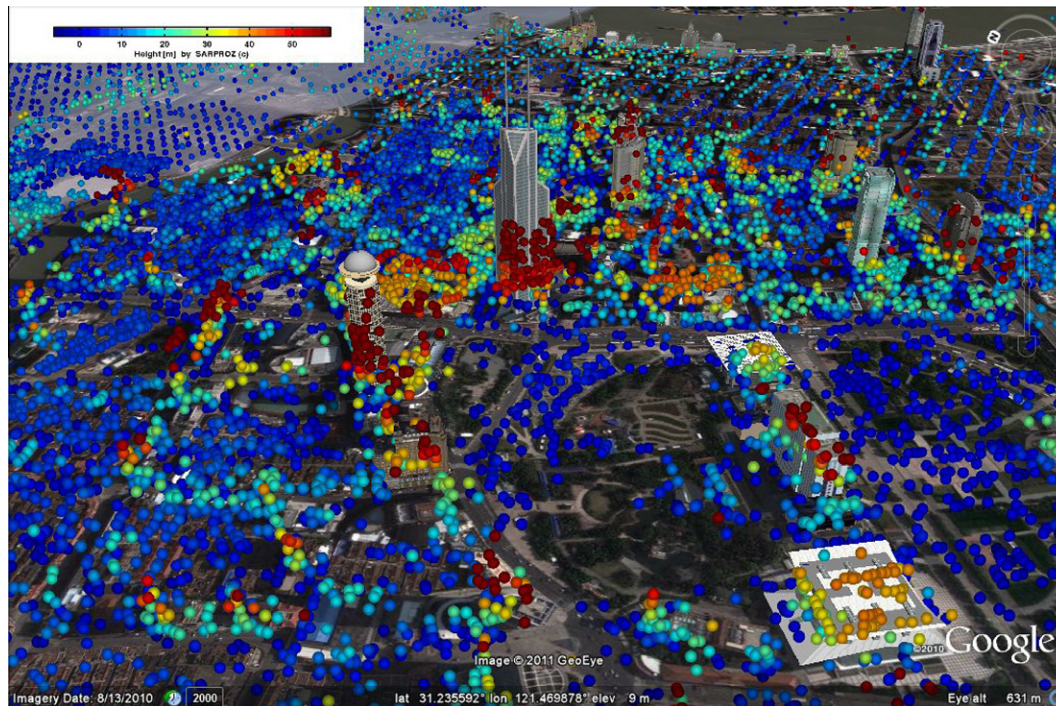


Fig. 4. 3D representation of PSs in Shanghai in Google Earth, together with 3D models of buildings. The color is proportional to the PS height, ranging [−5 60] m. (For interpretation of the references to color in this figure legend, the reader is referred to the web version of this article.)

estimated height, in a scale [−5 60] m. Yellow-red points are targets located at high level, and they reveal the vertical dimension of buildings in the image. The building models available in GE are displayed as well for the sake of comparison.

3.2. Subway tunnels identification

By looking at the subsidence overview estimated from Cosmo data in Fig. 3, one can start noticing several yellow linear features. In particular, we will focus the attention on a close up reported in Fig. 5, where the linear features have been made evident by color lines. To investigate the origin of the strips of subsidence, we retrieved from the online information of Shanghai Metro Company (Shanghai Metro Company, 2011) the location of the subway stations in the area and we placed corresponding marks in GE (the precise geolocation of the subway tunnels has not been released to the public). In Fig. 5a marks are labeled according to the line L and to the station sequence x as $L.x$. It is easy to notice that the marks plotted in Fig. 5a (corresponding to metro lines 7, 9, 10 and 11) fall exactly along the subsidence strips.

As a further cross-check, we analyzed the Shanghai subway network from the information we found online, as Google Maps (GMs). An example of comparison is shown in Fig. 6. What is very interesting to observe are the relative locations of the tunnels crossing the Huangpu River. In GM (image in Fig. 6a) the Fuxing East Road tunnel seems coinciding with the subway tunnel. From the optical image in GE (picture in Fig. 6b) one can see that the two entrances of the Fuxing East Road tunnel are in agreement with the tunnel location in GM. From the PSInSAR result (Fig. 6c), it is evident to observe that on the right side of the river the subway tunnel is north of the Fuxing East Road tunnel, revealing a clear error in GM. The reason is easily found by considering that the actual subway path is not known, so GM is only reporting lines connecting the subway stations.

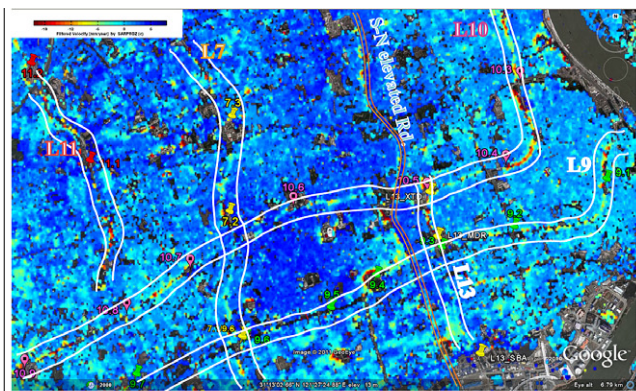
By comparing the subsidence rate of different subway lines in Fig. 5a, line 10 stands out as the one with strongest movements.

In particular, the subsidence along line 10 increases while approaching the west side of Huangpu River. Even though we have no proof that any connection with the detected motion exists, it is interesting to mention here that line 10 had several problems of water leakage, as reported in January 2011 (Wang and Zhuang, 2011), and a collapse between two trains happened in September 2011 (Mu, 2011).

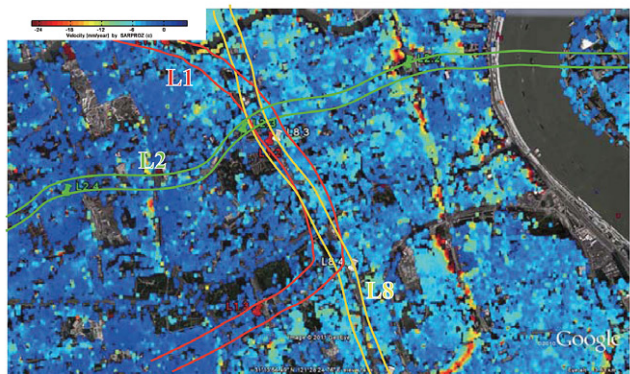
Along line 9 we note a particularly strong movement in correspondence of Dapuqiao station (9.4 in Fig. 5a). The border of the subsidence bowl is clearly identified, while in the middle no PS is visible. The middle of the subsidence bowl is in fact affected by noise derived from surface scattering changes, and no reliable deformation can be extracted. At the left of Station 9.4 along the subway path we have a lack of PS points. The reason for the absence of radar targets in that subway section is that the road right above, Zhaojiabang, is more than 60 m wide, and it is not offering any relevant reflection of the radar signal in the used Cosmo acquisition geometry.

It is now meaningful to analyze other subway lines in Shanghai to assess the actual probability of having targets along their path. Fig. 5b shows a close up taken from Fig. 5a around lines 1, 2 and 8. Such lines are not easily identified from the surface subsidence, however, the reason is not the lack of PSs but the absence of significant motion. We further investigated the remaining lines and we found that, in the analyzed area, the only tunnel section lacking of radar targets is the one below Zhaojiabang road. The outcome is quite important and it strengthens the InSAR reliability for urban tunnels monitoring.

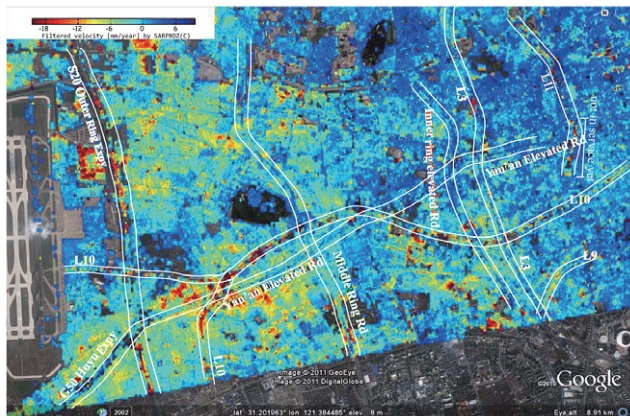
Finally, we carefully examined the detected motion of the subway lines in the analyzed area and we tried to investigate why some tunnels are subsiding and some others not. It is difficult to give an exhaustive interpretation of the result since no ground truth is available, however, we started analyzing the opening date of each subway line (the dates of tunnels excavation are not public). Fig. 7 lists all lines in Shanghai together with the date of service start. Leaving apart the subway lines not included in the



(a) Around new metro lines



(b) Metro old lines 1, 2 and 8, no motion is detected



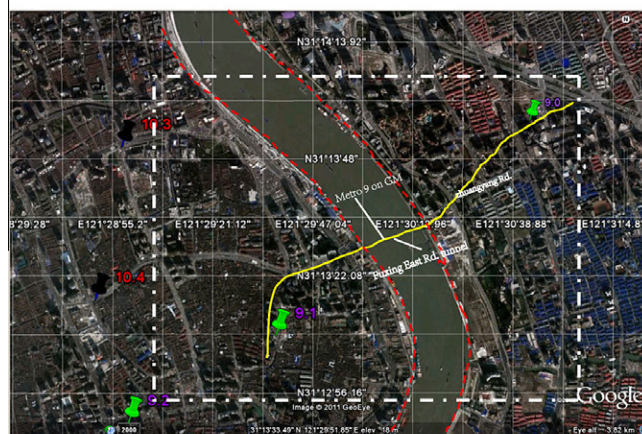
(c) Around the South-West of the analyzed area.

Fig. 5. Close up of the subsidence map in Shanghai. To highlight the subway path and other detected linear features, two color strips have been added at the sides of metro lines/roads. Placemarks are plotted in correspondence of subway stations and numbered in sequence according to the corresponding metro line (L7, L9, L10, L11 and L13). The red vertical strip of subsidence in (b) corresponding to line 10 appears evident. (For interpretation of the references to color in this figure legend, the reader is referred to the web version of this article.)

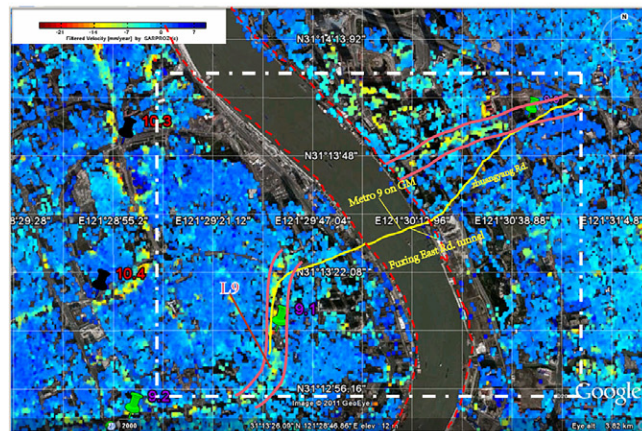
analyzed area, it is evident to observe that tunnels operative since 2007 or before do not show particular motion, while those opened from 2009 on appear clearly subsiding. It is important here to recall that the period we are analyzing with Cosmo spans one and half year from December 2008 to June 2010. With the current dataset, we cannot know if the old tunnels were affected by the same subsidence soon after the excavation and then stabilized in a couple of years. What we can state clearly is that all newly excavated tunnels are subsiding.



(a)



(b)



(c)

Fig. 6. Tunnel crossing the Huangpu river. From Google Maps (a) it seems that there is only 1 tunnel, shared by a road and by subway line 9. From optical data (b) we can assess that the tunnel position matches the road crossing the river. From the subsidence detected by PSInSAR (c), we see that the subway is crossing the river in a different position (Northern on the East side of the river).

3.3. Highways detection

By looking again at Fig. 5a, other strips of subsidence between line 7 and line 10 can be noticed, which we did not mention yet. The one on the right, starting from Station 10.3 and moving to South, is line 13, which is still under construction. Right to its left

opening Date	Apr.95	Sep.99	Dec. 00	Sep.07	Dec.07	Mar.09	Jul.09	Dec.09	Feb.10	Mar. 10	Apr. 10	May.10
MTR lines												
L1(Shanghai railway station - Jinjiang Park)	stable											
L2(Zhongshan Rd. - Longyang Rd.)	stable											
L3(Shanghai South railway station - Jiangwan Town)	stable											
L4(Damuqiao - damuqiao, circle)	stable											
L6(Gangcheng Rd. - Wulian Rd. station)	stable											
L8(Shiguang Rd. - Yaohua Rd. station)	stable											
L9.1(Songjiang New town station - Guilin Rd. station)	outside the analyzed area											
L13(Madang Rd. - Changqing Rd.)	Subsiding											
L13(Danshui Rd./XintianDi-Madang Rd.)	Subsiding											
L7.1 (Qihua Rd. - Huamu Rd.)	outside the analyzed area											
L9.2(Yishan Rd. - Century Avenue)	Subsiding											
L9.3 (Yishan - Songjiang New town)	outside the analyzed area											
L7.2(Shanghai University - Huamu Rd. station)	Subsiding											
L11.1(Jiangshu Rd. - Jiading North)	Subsiding											
L9.3(Xuhui - Yanggaozhong)	Subsiding											
L10(east part from Longxi Rd. station)	Subsiding											

Fig. 7. Opening timetable of metro lines in Shanghai. Lines opened before 2009 are now stable, while new lines, opened from 2009 on, appear as subsiding during the analyzed time span.

we notice another series of slightly subsiding areas displaced vertically in the figure. By observing in detail the corresponding optical image in GE, one can realize that those points are aligned beside the South–North elevated Road. However, the elevated road itself appears as blue in the subsidence map. What is subsiding are the buildings aside.

Several other similar behaviors can be noticed in the South–West part of the analyzed area, reported in Fig. 5c. In Fig. 5c, starting from the right, we firstly see the subsiding tunnel of line 10, passing the whole picture from East to West, and splitting up into two different branches on the left, one heading westward to Hongqiao airport and the second one to the South. Then, still on the right, we see two sections of lines 11 and of line 9. Next to them we have two vertical linear features, corresponding to line 3 and to the Inner Ring Elevated Road. Both strips show up as blue, in neat contrast with the surroundings, which appear between yellow and light blue. As for the South–North elevated Road in Fig. 5a, we are in front of linear structures that are more stable than the surrounding areas. All these structures (both road and metro lines) have in common to be elevated.

Next to the middle of Fig. 5c, vertically in the image, we have the Middle Ring Road. Its track appears in turns stable (blue) or moving consistently with the terrain around (yellow). Such road is in fact partly at ground level and partly underground. Most underground sections appear as subsiding. Finally, at the left of Fig. 5c, before Hongqiao airport, we can distinguish the S20 Outer Ring Expressway, which is clearly affected by subsidence at intervals. In this case, the road is at ground level, and we did not find yet a clear explanation for its motion, if not the soft clay characterizing the Shanghai substratum.

3.4. Subsidence profile of metro tunnels

The density of PSs in X band in urban sites is so high to make it possible distinguishing the displacement of single roads, highways, subway lines. Even more, by observing accurately some subsiding sections in Fig. 5a–c, one can clearly distinguish the progression of colors from blue to red, passing from yellow and intermediate shades. We decided then to try to estimate the subsidence profile of some segments of the Shanghai metro tunnels, to gain more information on the ongoing settlement.

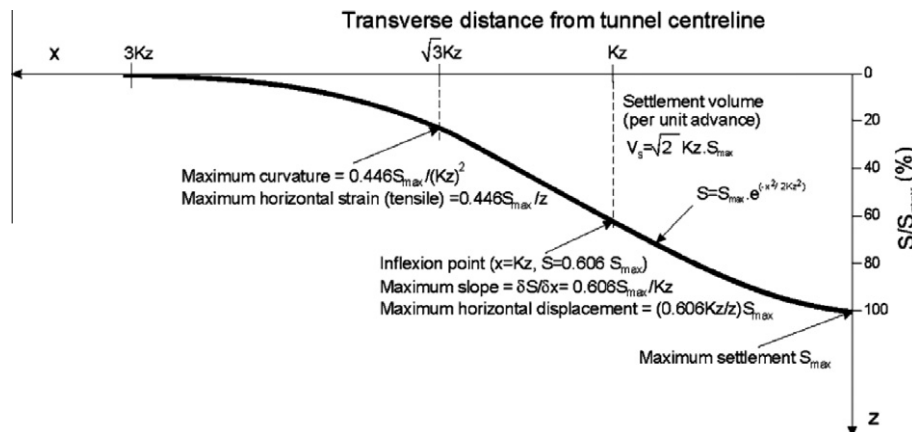


Fig. 8. Idealized transverse settlement profile induced by tunnel excavation (Mahmutoğlu, 2011).

This study is quite unique in its nature. Usually, settlement induced by tunnel excavation is analyzed either as a function of the transverse coordinate (settlement profile) or as a function of time (to study transients and stabilization). In our case, we have an average deformation trend (a linear transient) as a function of the transverse coordinate. We approach it starting from the existing literature.

The analysis of the settlement transverse profile induced by tunneling has been considerably simplified by (Martos, 1958) and (Peck, 1969), who proposed to approximate the subsidence derived from a single tunnel excavation with a Gaussian curve. (O'Reilly and New, 1982) related the subsidence to the ground conditions through an empirical “trough width parameter” and got an idealized settlement curve, shown in Fig. 8 (Mahmutoglu, 2011). In Fig. 8, the x axis is the transverse distance from the tunnel centre, the z axis is the normalized subsidence S/S_{max} and K_z is the “trough width parameter”. S_{max} and K_z are the two key parameters that model the shape of the idealized subsidence curve, and they depend on tunnel and terrain characteristics, as well as on the excavation technology. Finally, in the case of twin tunnels, if the distance between them is higher than the diameter of the single tunnels, the profile is still gaussian and the settlement trough can be approximated as the sum of two troughs.

As far as the time coordinate is considered, the settlement trend induced by tunneling has often been approximated with hyperbolic models (Hwang and Moh, 2006). However, recent studies have shown that the settlement can be far more complex, but well approximated by linear segments (Hwang and Moh, 2006). In particular, during the excavation and in the subsequent days the highest displacement takes place, and then the slow terrain consolidation can last till one, two or even three years.

In our test-site we chose as best cases a section of line 9 close to Xiaonanmen Station (9.1 in Fig. 5a) and a section of line 10 close to Laoximen Station (10.4 in Fig. 5a). In the extracted sections (about 200 m long) the subway goes straight and the deformation pattern is homogeneous, so that we can observe the transverse subsidence curve by stacking the deformation trend along the main tunnel axes. Fig. 9 shows the two analyzed sections along the transverse

coordinate, together with a Gaussian curve fitting the data points. The profile shape is quite in accordance with the theoretical model.

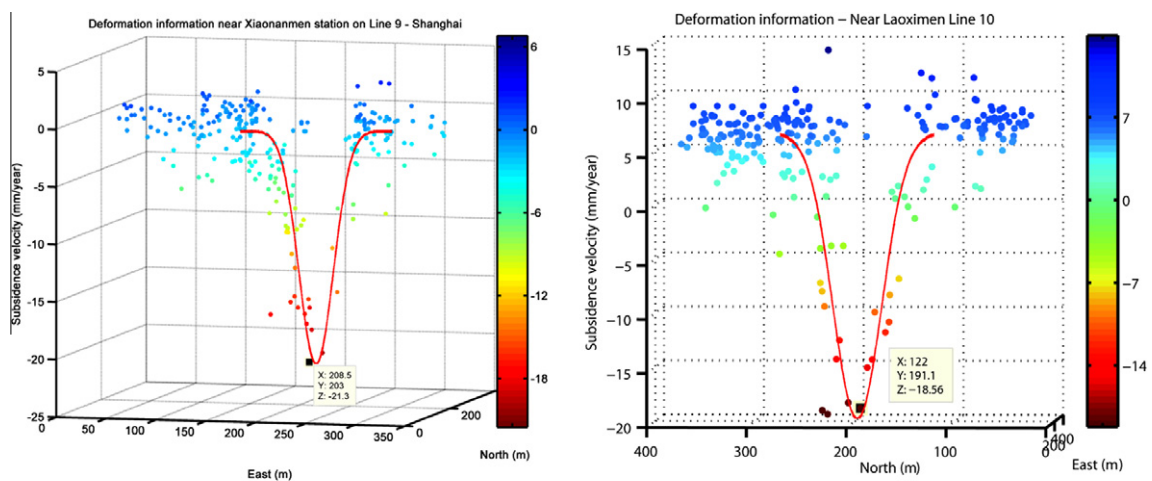
To quantify the expected width of the profile, we base our analysis on the tunnel information we found in the literature. Yang (Yang et al., 2010) studied several tunneling cases in Shanghai, and he found an empirical relationship between tunnel radius and the trough width K_z . Reference (Fu et al., 2010; Hu et al., 2003; Lu et al., 2007) published some numbers relative to lines 9 and 10, which have very close characteristics. In particular, the tunnel diameter is given as 6.2 m, and an indicative distance between parallel tunnels is said being 19 m. According to the given numbers, the profile of the surface deformation should have a trough of about 20 m and consequently an overall width of about 80 m, which is in good accordance with the profiles shown in Fig. 9.

To conclude, the maximum deformation trend measured from Fig. 9 is in the order of 20 mm/year for line 10 and 18 mm/year for line 9 in a time span of about one year and half. Even without knowing precisely when the tunnels were excavated, being the metro lines operative since April 2010, we can reasonably assume to observe their very first year of life. The linear approximation holds and we can in this way assess the descriptive parameters of the linear subsidence profile.

3.5. Tunnel subsidence and high buildings

The study of the transverse subsidence profile carried out in the previous subsection is extremely important to assess building damage in the areas close to the subway path. Moreover, retrieving the subsidence model parameters, even if with approximation, is very useful to predict movements where PS targets are missing. No serious consequences should happen if a road overlaying a subway tunnel subsides. However, if buildings lie over the settling terrain, it may suffer damages, and authorities must be able to quantify the risk and take appropriate decisions to protect the population from possible accidents.

The work here conducted should bring enough arguments to convince about the convenience of using multi-temporal high-resolution InSAR analysis for monitoring urban sites, in particular for



(a) Transverse subsidence profile near Xiaonanmen station on Line 9 (line:1180-1230, sample:16750-16950, around 100 meters length of subway line), color ranging between -18 and 7mm/year

(b) Transverse subsidence profile near Laoximen station, Line 10, color ranging between -20 and 14mm/year

Fig. 9. Subsidence trend profiles of metro lines 9 and 10 in Huangpu District. The vertical axis as well as the color display the settlement velocity in mm/years. The Horizontal axis is expressed in meters in UTM coordinates. (For interpretation of the references to color in this figure legend, the reader is referred to the web version of this article.)

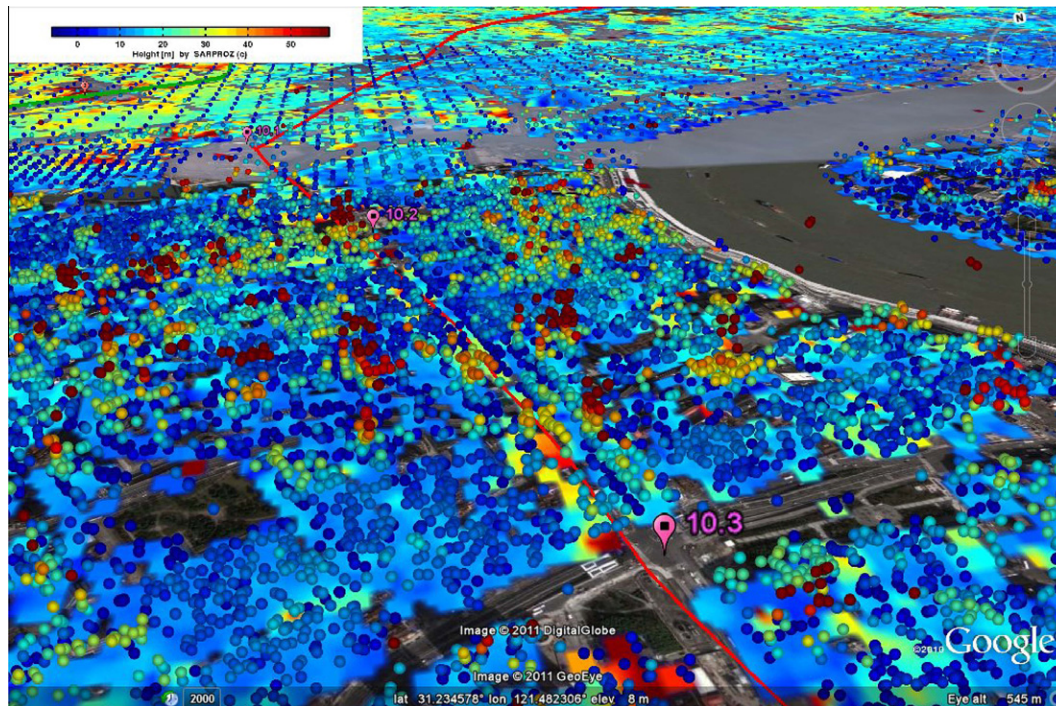


Fig. 10. 3D location of PSs (plotted with dots, color proportional to height, [0 60] m) integrated with subsidence map (bottom layer, the color showing the subsidence rate [−20 5] mm/year). (For interpretation of the references to color in this figure legend, the reader is referred to the web version of this article.)

fast developing environments like China. Before concluding, we exploit the capabilities of the technique here described to highlight two possible risky situations.

As previously shown, the PS technique is able to estimate both the deformation trend and the location of the targets. We can combine the two estimates, together with the subway tunnels analysis, to identify high-rise buildings affected by movement on the subway path. Fig. 10 shows an example along line 10 in the Huangpu district. In Fig. 10 we displayed at the same time the detected subsidence map (as GE ground overlay) and the 3D location of PSs (plotted with dots). The color scale of the ground overlay shows the deformation trend, while the dots color is proportional to their height. In this way, we can observe that, close to station 10.3 and going to the North, we have a couple of 40m or more buildings affected by about 15 mm/year displacement.

Another example of building affected by the subway settlement (not reported in Fig. 10) has been identified in the South East of the analyzed area. By looking at Fig. 5c, the building is located after the Y splitting of line 10 approaching the airport, North of Yan'an elevated road.

4. Conclusions

In this work we have shown the great performances offered by the PS technique applied to an X band SAR datasets in an urban area like Shanghai to monitor with unprecedented details ground settlements. In particular, 33 SAR images acquired by the Italian sensor Cosmo-SkyMed have been processed with the SARPROZ software, and more than 1.2 million of independent Persistent Scatterers have been detected in Shanghai in about 600 sq km. The displacement trend estimated from the targets reveals the subsidence of Shanghai with impressive details, making it possible to track the path of newly excavated subway tunnels by looking at the overlying surface motion. On the other side, elevated highways stand out showing higher stability than the surrounding terrain. The density of detected targets is so high to allow studying the transverse subsidence profile over metro tunnels, which is useful

to predict possible building damage. The targets estimated height is then used to identify high buildings close to the subway path affected by settlement and to identify possible risky areas. High-resolution multi-temporal InSAR analysis show in this way to be extremely useful to detect and to predict urban surface displacement for civil protection purposes.

Acknowledgements

Cosmo-SkyMed data used in this project have been provided by Eastdawn, Beijing. Part of the costs have been covered by the CUHK Direct Grant fund, Project ID 2021066, “Subsidence analysis and DEM estimation in China by means of repeated X band Cosmo-SkyMed images”. Hardware was supported by Spatial Technologies, Hong Kong. This work was partially supported by the Research Grants Council (RGC) General Research Fund (GRF) (Proj. Ref. No. 415911) of HKSAR.

References

- Colesanti, C., Ferretti, A., Perissin, D., Prati, C., Rocca, F., 2003. Evaluating the effect of the observation time on the distribution of SAR permanent scatterers. In: Proceedings of FRINGE 2003, Frascati, Italy, 1–5 December, ESA SP – 550.
- Damoah-Afari, P., Ding, X., Lu, Z., Li, Z.W., 2008. Detection ground settlement of Shanghai using interferometric synthetic radar (InSAR) techniques. The International Archives of the Photogrammetry, Remote Sensing and Spatial Information Sciences 37 (Part B7), 117–124.
- Damoah-Afari, P., Ding, X., Lu, Z., Li, Z.W., Omura, M., 2007. Six years of land subsidence in Shanghai revealed by JERS-1 SAR data. In: Sensing and Understanding Our Planet, International Geoscience and Remote Sensing Symposium 2007 (IGARSS07), Barcelona, Spain, 23–27 July, p. 5 (on CD-ROM).
- Fu, D.M., Li, B.H., Ma, Z.Z., 2010. On construction technique of soft soil shield cutting directly reinforce concrete pile foundation. China Municipal Engineering 4, 46–47 (Chinese).
- Ferretti, A., Bianchi, M., Prati, C., Rocca, F., 2005. Higher-order permanent scatterers analysis. EURASIP Journal on Advances in Signal Processing 2005 (12), 3231–3242.
- Ferretti, A., Prati, C., Rocca, F., 2000. Nonlinear subsidence rate estimation using permanent scatterers in differential SAR interferometry. IEEE Transaction on Geoscience and Remote Sensing 38 (5), 2202–2212.
- Ferretti, A., Prati, C., Rocca, F., 2001. Permanent scatterers in SAR interferometry. IEEE Transaction on Geoscience and Remote Sensing 39 (1), 8–20.

- Gong, S.L., Li, C., Yan, S.L., 2009. The microscopic characteristics of Shanghai soft clay and its effect on soil body deformation and land subsidence. *Environmental Geology* 56 (6), 1051–1056.
- Gov.cn, 2011. Shanghai makes progress staying high and dry. <http://english.gov.cn/2007-02/06/content_519239.htm> (accessed 9.7.2012).
- Hu, R., Yue, Z., Wang, L., Wang, S.J., 2004. Review on current status and challenging issues of land subsidence in China. *Engineering Geology* 76 (1–2), 65–77.
- Hu, Z., Yue, Z., Zhou, J., Tham, L., 2003. Design and construction of a deep excavation in soft soils adjacent to the Shanghai metro tunnels. *Canadian Geotechnical Journal* 40 (5), 933–948.
- Hwang, R.N., Moh, Z.C., 2006. Prediction of long-term settlements induced by shield tunneling. *Journal of GeoEngineering* 1 (2), 63–70.
- Li, T., Liu, J.N., Liao, M.S., Kuang, S.J., Lu, X., 2004. Monitoring city subsidence by D-InSAR in Tianjin area. In: *IEEE International Geoscience and Remote Sensing Symposium (IGARSS)*, vol. 5, Anchorage, Alaska, 20–24 September, pp. 3333–3336.
- Liu, G., Wu, J., Li, J., Chen, Q., Qin, J., Zhang, H., Zhang, R., Jia, H., Luo, X., 2009. Mapping surface deformation related to the 2008 Wenchuan earthquake with ALOS InSAR and GPS observations. In: *Proceedings of the SPIE*, vol. 7471, Berlin, Germany, 31 August–3 September, pp. 74711N–74711N–8.
- Lu, M., Qin, H., Zhu, Z.X., 2007. Introduction of shield running tunnel emergency repair of Shanghai rail rapid transit line 9. *China Building Waterproofing* 1, 63–70 (Chinese).
- Mahmutoglu, Y., 2011. Surface subsidence induced by twin subway tunnelling in soft ground conditions in Istanbul. *Bulletin of Engineering Geology and the Environment* 70 (1), 115–131.
- Martos, F., 1958. Concerning an approximate equation of the subsidence trough and its time factors. In: *International Strata Control Congress, Leipzig*. Deutsche Akademie der Wissenschaften zu Berlin, Section für Bergbau, Berlin, pp. 191–205.
- Miller, P.F., Vandome, F.A., McBrewhster, J., 2010. *Shanghai Metro*, VDM Verlag Dr. Mueller e.K., ISBN: 6134141208, 9786134141208.
- Monjoie, A., Paepe, R., Su, H.Y., 1992. Land subsidence in Shanghai (R.P. of China). *Bulletin of Engineering Geology and the Environment* 46 (1), 3–5.
- Mu, X.Q., 2011. Two subway trains collide in shanghai, over 270 injured. <http://news.xinhuanet.com/english2010/china/2011-09/27/c_131163517.htm> (accessed 9.6.2012).
- O'Reilly, M.P., New, B.M., 1982. Settlements above tunnels in the United Kingdom – their magnitude and prediction. In: *Proceedings of Tunnelling, Institute of Mining Metallurgy*, London, pp. 173–181.
- Osmanoglu, B., Dixon, T.H., Wdowinski, S., Cabral-Cano, E., Jiang, Y., 2010. Mexico city subsidence observed with persistent scatterer InSAR. *International Journal of Applied Earth Observation and Geoinformation* 13 (1), 1–12.
- Peck, R.B., 1969. Deep excavations and tunnelling in soft ground. In: *7th International Conference on Soil Mechanics and Foundation Engineering*, vol. 7(3), 22–23 October, Mexico, pp. 225–290.
- Perissin, D., 2011. SARPROZ manual. <http://ihome.cuhk.edu.hk/b122066/index_files/download.htm> (accessed 9.6.2012).
- Perissin, D., Rocca, F., 2006. High accuracy urban DEM using permanent scatterers. *IEEE Transactions on Geoscience and Remote Sensing* 44 (11), 3338–3347.
- Perissin, D., Wang, T., 2010. Time series InSAR applications over urban areas in China. *IEEE Journal of Selected Topics in Applied Earth Observations and Remote Sensing* 4 (1), 92–100.
- Perissin, D., Wang, Z., Wang, T., 2011. The SARPROZ InSAR tool for urban subsidence/manmade structure stability monitoring in China. In: *Proceedings of ISRSE 2011*, Sidney, Australia, 10–15 April.
- Perissin, D., Wang, T., 2012. Repeat-pass SAR interferometry with partially coherent targets. *IEEE Transactions on Geoscience and Remote Sensing* 50 (1), 271–280.
- Shanghai Metro Company, 2011. Map of information around the metro station, Dec. 2011. <www.shmetro.com> (accessed 9.6.2012).
- Shanghai.gov.cn, 2007. City stays above 'the sea' but only just. <<http://www.shanghai.gov.cn/shanghai/node17256/node18151/userobject22ai26540.html>> (accessed 9.6.2012).
- Shi, L.X., Bao, M.F., 1984. Case history No. 9.2 Shanghai. In: Poland, Joseph F.(Ed.), *Guidebook to studies of land subsidence due to groundwater withdrawal*, United Nations Educational, Scientific and Cultural Organization, Paris, pp. 155–160.
- Tang, Y.Q., Yang, P., Zhao, S.K., Zhang, X., Wang, J.X., 2008. Characteristics of deformation of saturated soft clay under the load of Shanghai subway line No. 2. *Environmental Geology* 54 (6), 1197–1203.
- Wang, J.H., Zhuang, J., 2011. Water leakage happened on more than half of stations on metro line 10 in Shanghai. <<http://news.sina.com.cn/c/p/2011-01-17/174121829833.shtml>> (Chinese, accessed 9.6.2012).
- Wei, G., Chen, W.J., Wei, X.J., 2011. Prediction of surface settlement induced by double-o-tube shield tunnel excavation (Chinese). *Rock and Soil Mechanics* 32 (4), 7–11.
- Water news Online, U.S., 2007. Shanghai claims progress in fighting subsidence; taking special measures for subways. <<http://www.uswaternews.com/archives/arcglobal/7shanclai2.html>> (accessed 10.4.2012).
- Yang, T.L., Yan, X.X., Wang, H.M., Zhan, L.X., 2010. Study on engineering land subsidence caused by shield construction in subway tunnel (Chinese). *Shanghai Geology* 31, 7–11.
- Zebker, H.A., Villasenor, J., 1992. Decorrelation in interferometric radar echoes. *IEEE Transaction on Geoscience and Remote Sensing* 30 (5), 950–959.